Supplement of The Cryosphere, 14, 4121–4133, 2020
https://doi.org/10.5194/tc-14-4121-2020-supplement

The Cryosphere Open Access EGU

Supplement of

Sharp contrasts in observed and modeled crevasse patterns at Greenland's marine terminating glaciers

Ellyn M. Enderlin and Timothy C. Bartholomaus

Correspondence to: Ellyn M. Enderlin (ellynenderlin@boisestate.edu)

1 Figures

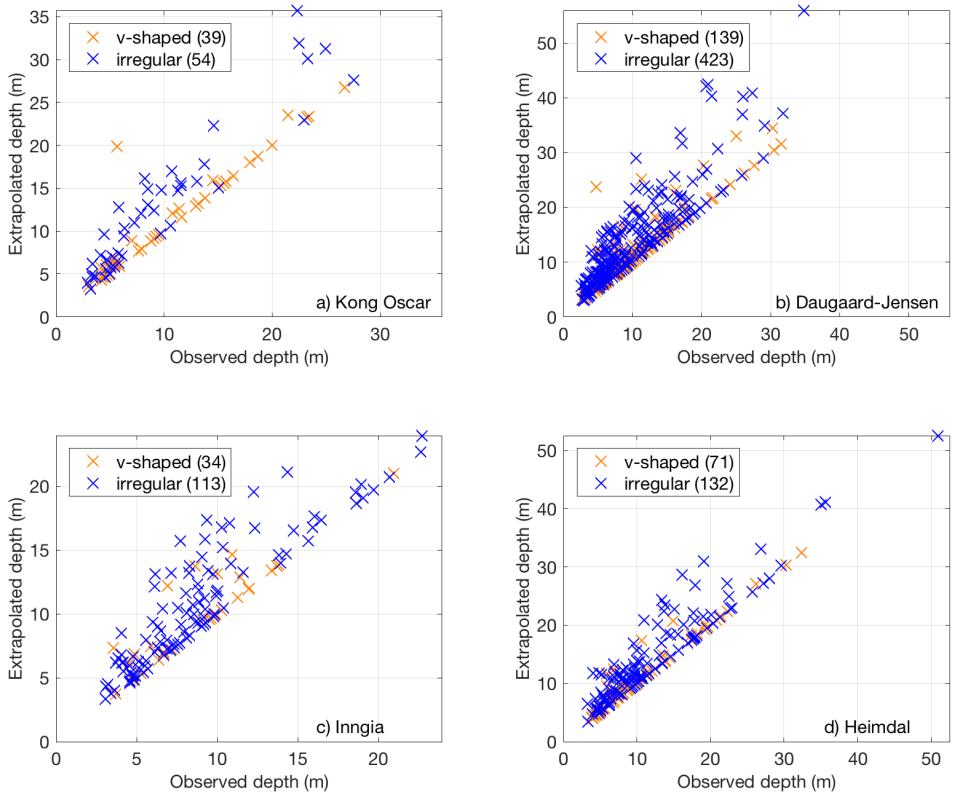

Figure S1: Crevasse depth estimates from surface elevation observations (observed depths) plotted against depth estimates using extrapolated using crevasse wall slopes (extrapolated depths). The number of each type of crevasse is listed in the legends. a) Data from Kong Oscar Gletsjer. b) Data from Daugaard-Jensen Gletsjer. c) Data from Inngia Isbræ. d) Data from Heimdal Gletsjer.

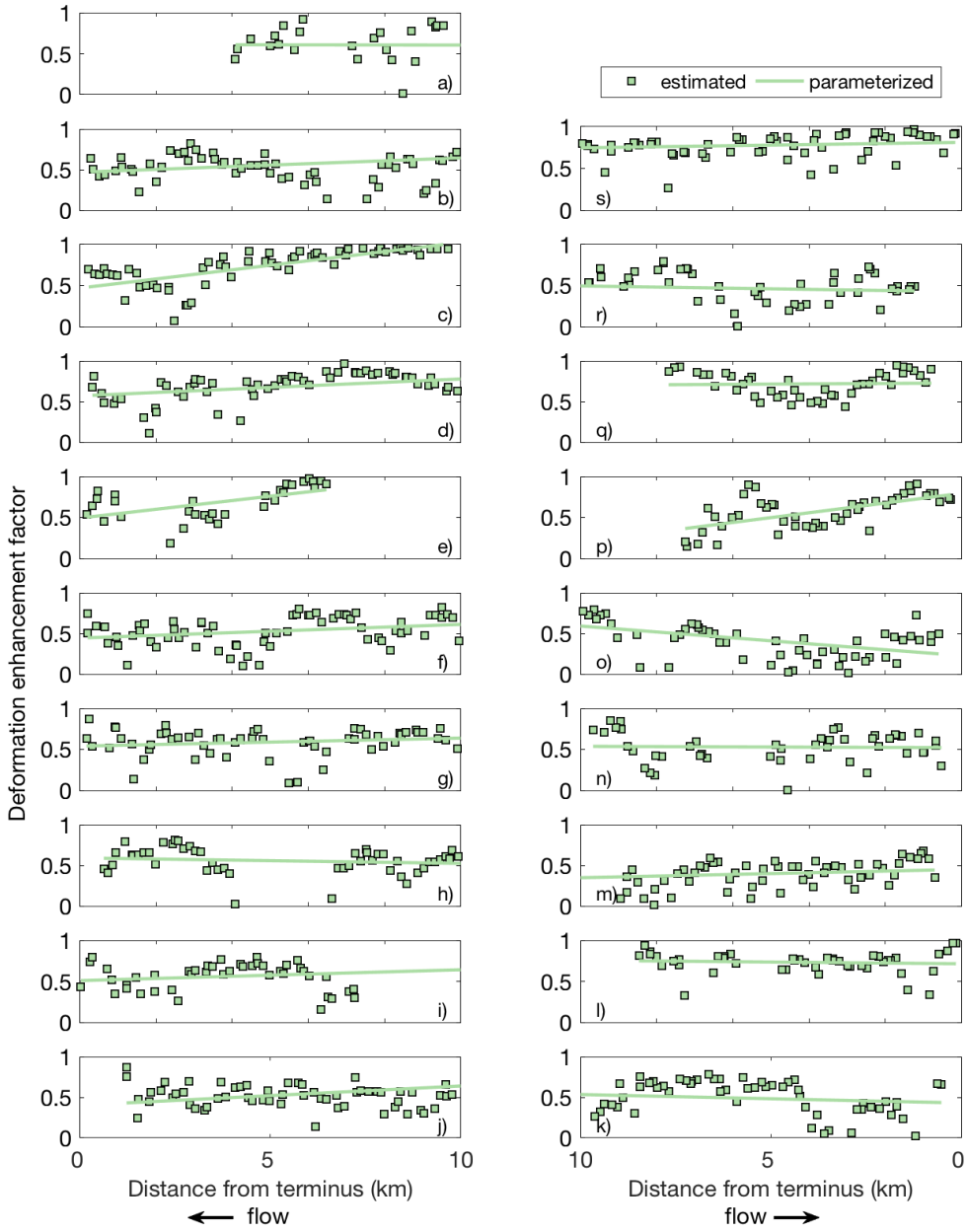

Figure S2: The deformation enhancement factor inferred from the misfit between observed crevasse depths and depths modeled plotted along flow. Panels are geographically arranged so that western glaciers are on the left and eastern glaciers are on the right. Common names (Greenlandic names) are a) Ryder Gletsjer, b) Harald Moltke Bræ (Ullip Sermia), c) Kong Oscar Gletsjer (Nuussuup Sermia), d) Illiup Sermia, e) Upernavik North Isstrøm, f) Upernavik

Isstrøm (Sermeq), g) Inngia Isbræ (Salliarutsip Sermia), h) Umiammakku Sermiat, i) Rink Isbræ (Kangilliup Sermia), j) Jakobshavn Isbræ (Sermeq Kujalleq), k) Heimdal Gletsjer, l) Koge Bugt Gletsjer, m) Helheim Gletsjer, n) Midgård Gletsjer, o) Kangerlussuaq Gletsjer, p) Dendrit Gletsjer, q) Magga Dan Gletsjer, r) Daugaard-Jensen Gletsjer, s) Zachariae Isstrøm.

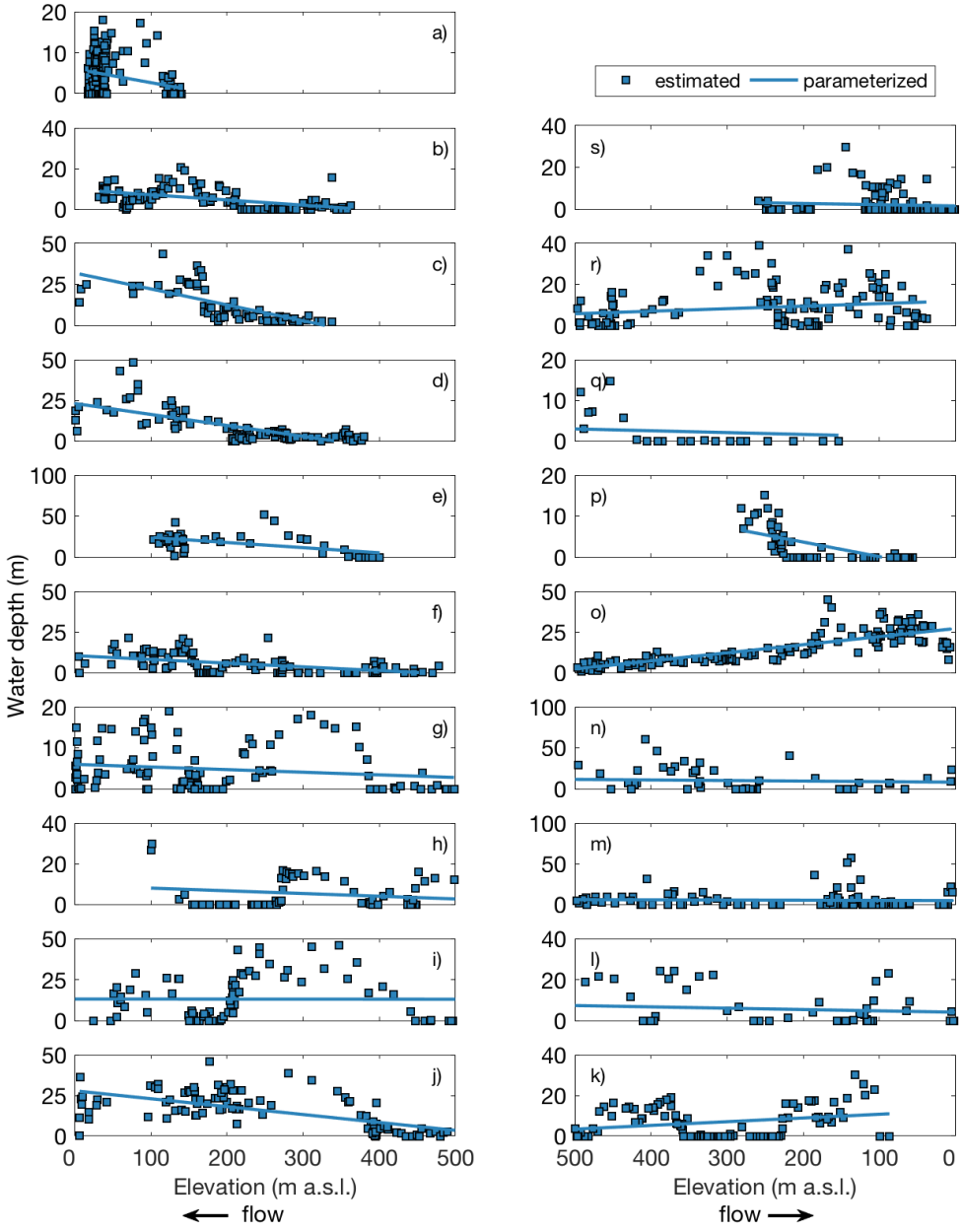

Figure S3: Water depths in crevasses inferred from the misfit between observed crevasse depths and depths modeled with a constant deformation enhancement factor plotted against surface elevation. Panels are organized geographically, as in Figure S2.

5

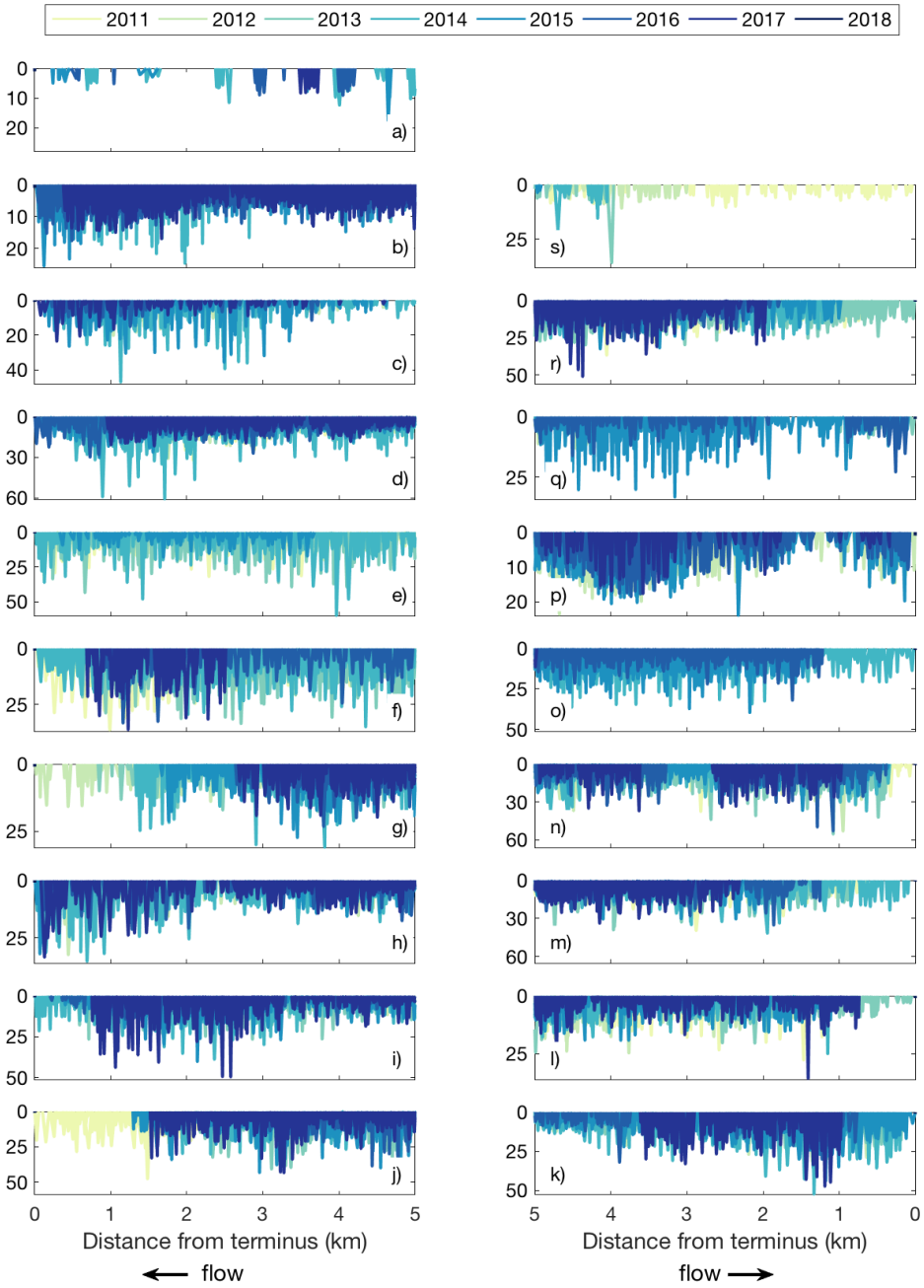

Figure S4: Time series of observed crevasse depths over the seaward-most 5km of each glacier. The colors correspond to the years listed in the legend. Panels are organized geographically, as in Figure S2.

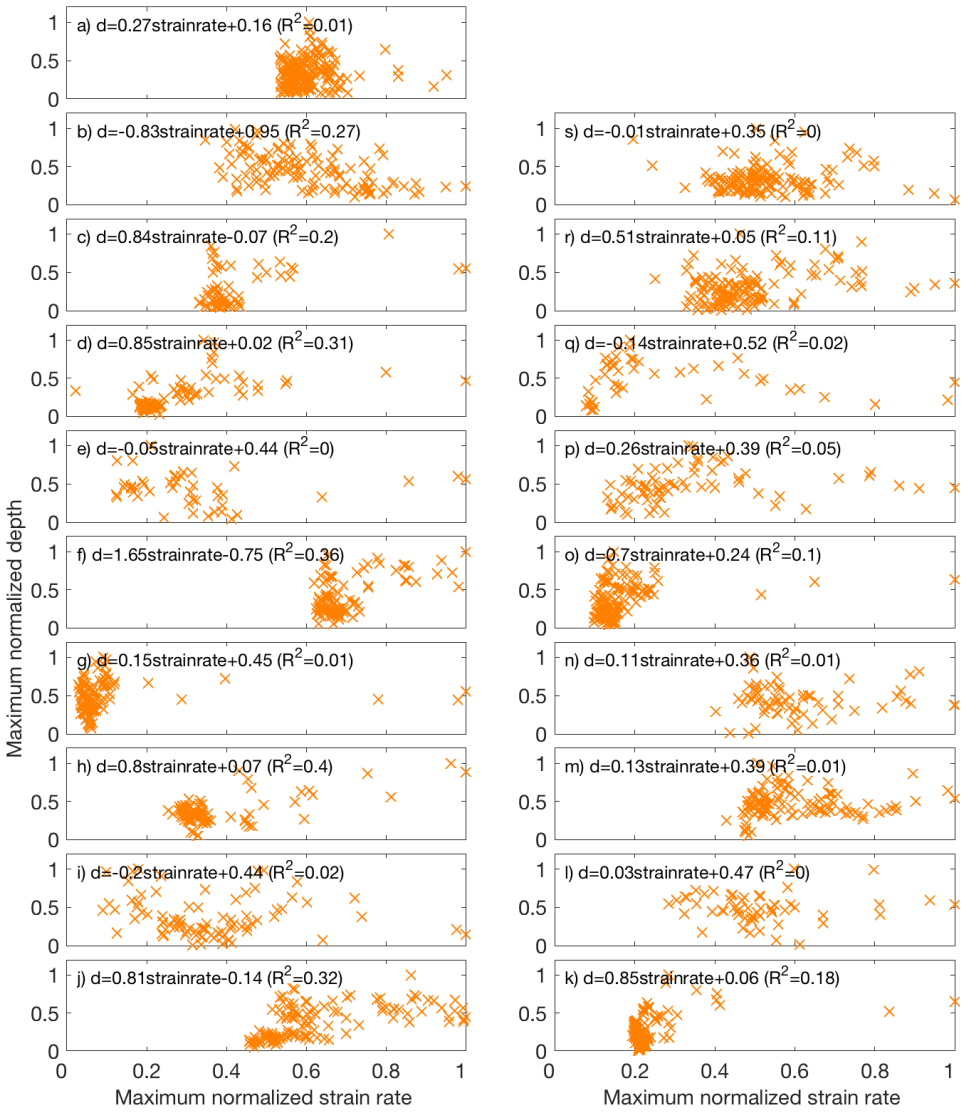

Figure S5: Profiles of normalized strain rate and maximum normalized observed crevasse depth. The equation for the best-fit linear polynomial, including the correlation coefficient, is included in the plot for each glacier.

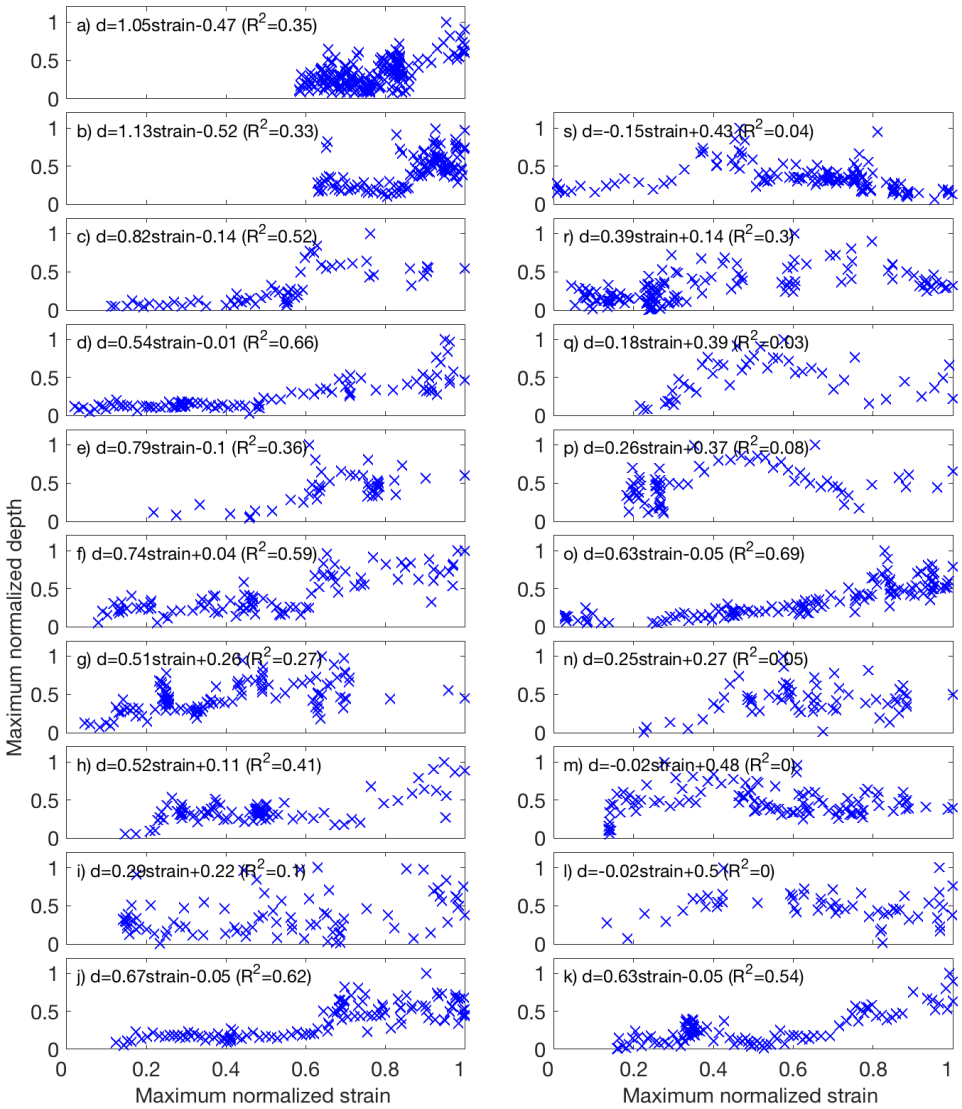

Figure S6: Profiles of normalized strain and maximum normalized observed crevasse depth. The equation for the best-fit linear polynomial, including the correlation coefficient, is included in the plot for each glacier.

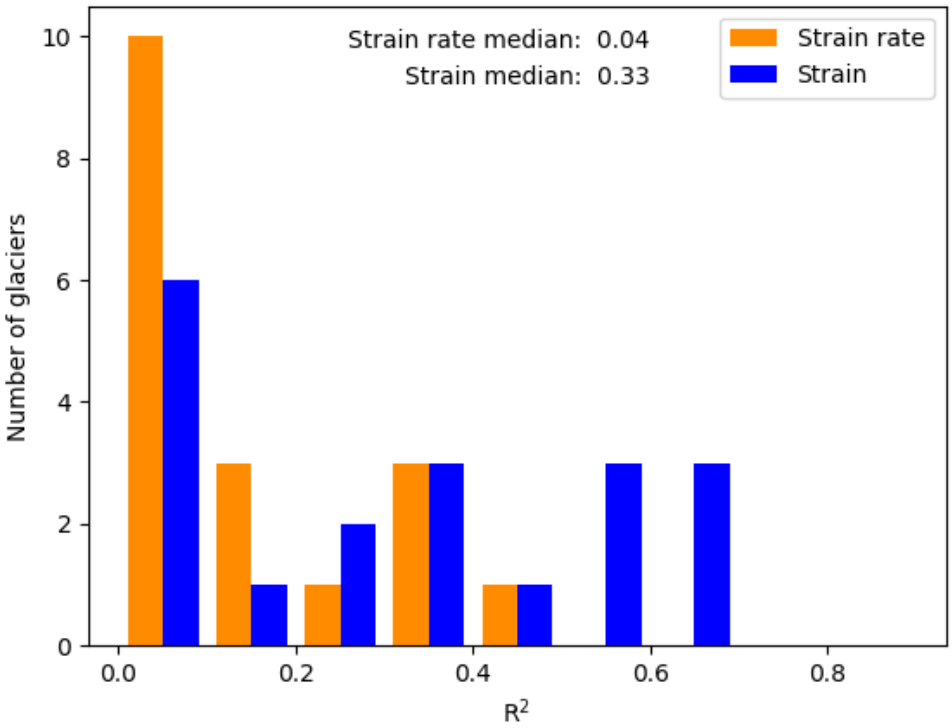

Figure S7: Evaluation of the relationships between strain rate and crevasse depth, and strain and crevasse depth, summarizing individual-glacier relationships shown in Figs. S5 and S6. Histograms show the goodness of fit for ordinary least square linear relationships in which normalized, observed crevasse depths are predicted with normalized strain rates (orange) or normalized strain (blue) for all glaciers.

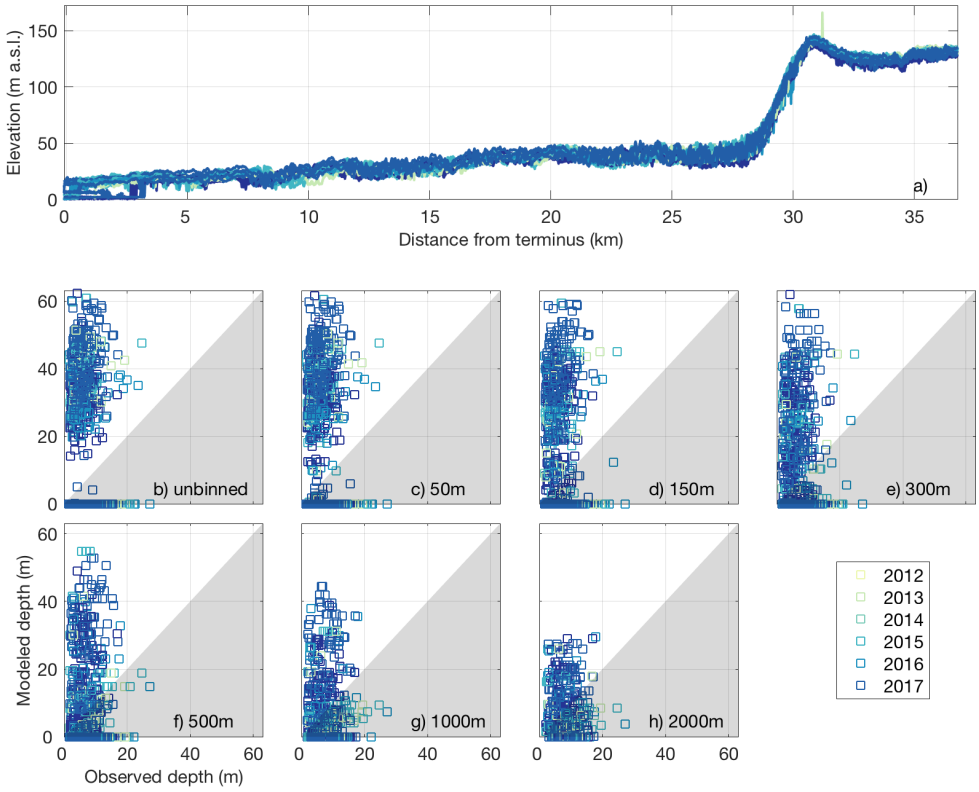

Figure S8: Ryder Gletsjer crevasse depth data. The legend indicates the observation year for all panels. a) Elevation profile time series extracted along the Operation IceBridge swath. b-h) Scatterplots of observed crevasse depths plotted against modeled crevasse depths. Points that fall in the white (gray) region represent model over-estimates (under-estimates) of the observed depths. All observations are shown in b whereas the maximum observed and median modeled depths within along-flow bins are shown in c-h, with bin sizes ranging from 50-2000m.

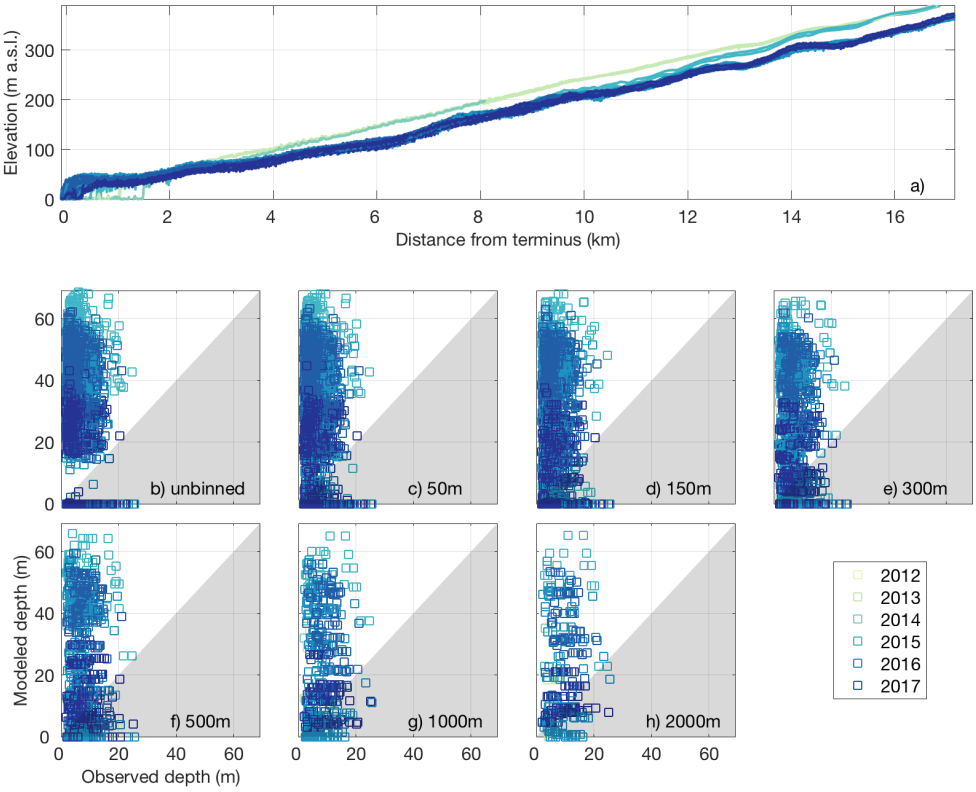

Figure S9: Harald Moltke Bræ (Ullip Sermia) crevasse depth data. The legend indicates the observation year for all panels. a) Elevation profile time series extracted along the Operation IceBridge swath. b-h) Scatterplots of observed crevasse depths plotted against modeled crevasse depths. Points that fall in the white (gray) region represent model over-estimates (under-estimates) of the observed depths. All observations are shown in b whereas the maximum observed and median modeled depths within along-flow bins are shown in c-h, with bin sizes ranging from 50-2000m.

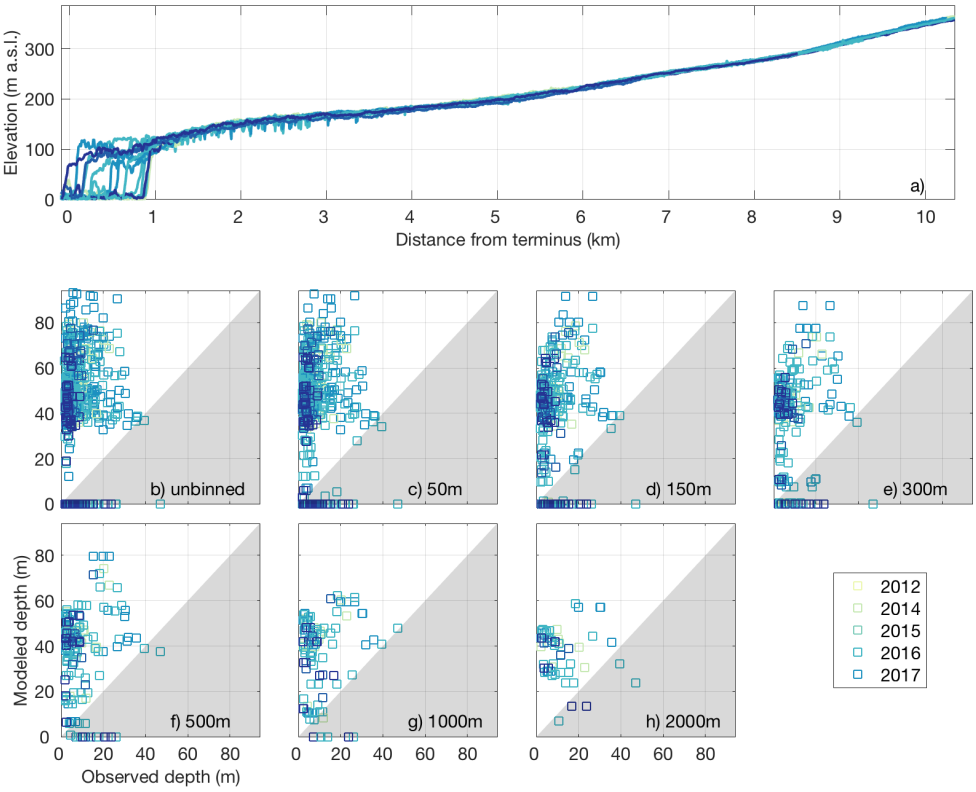

Figure S10: Kong Oscar Gletsjer (Nuussuup Sermia) crevasse depth data. The legend indicates the observation year for all panels. a) Elevation profile time series extracted along the Operation IceBridge swath. b-h) Scatterplots of observed crevasse depths plotted against modeled crevasse depths. Points that fall in the white (gray) region represent model over-estimates (under-estimates) of the observed depths. All observations are shown in b whereas the maximum observed and median modeled depths within along-flow bins are shown in c-h, with bin sizes ranging from 50-2000m.

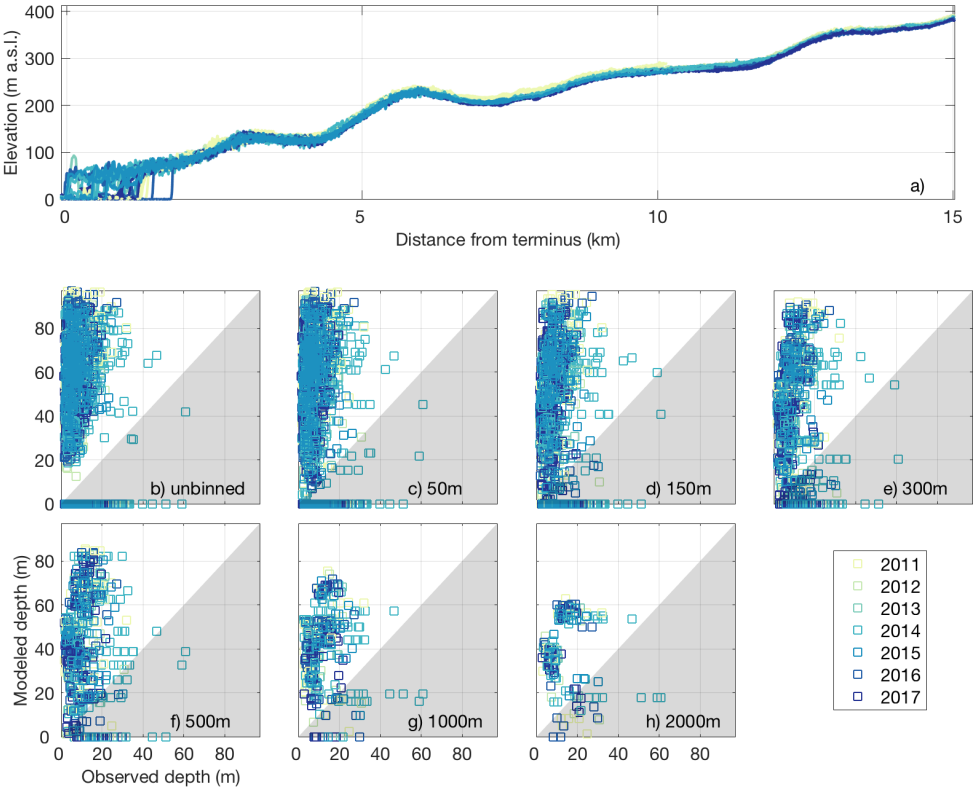

Figure S11: Illullip Sermia crevasse depth data. The legend indicates the observation year for all panels. a) Elevation profile time series extracted along the Operation IceBridge swath. b-h) Scatterplots of observed crevasse depths plotted against modeled crevasse depths. Points that fall in the white (gray) region represent model over-estimates (under-estimates) of the observed depths. All observations are shown in b whereas the maximum observed and median modeled depths within along-flow bins are shown in c-h, with bin sizes ranging from 50-2000m.

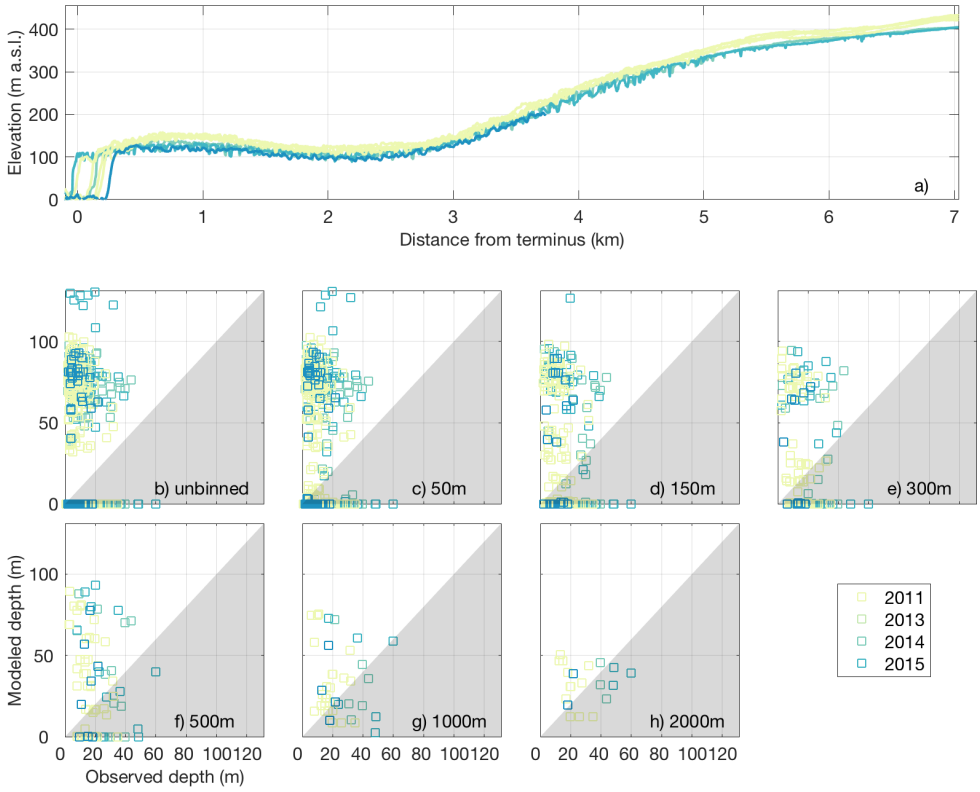

Figure S12: Upernavik North Isstrøm crevasse depth data. The legend indicates the observation year for all panels. a) Elevation profile time series extracted along the Operation IceBridge swath. b-h) Scatterplots of observed crevasse depths plotted against modeled crevasse depths. Points that fall in the white (gray) region represent model over-estimates (under-estimates) of the observed depths. All observations are shown in b whereas the maximum observed and median modeled depths within along-flow bins are shown in c-h, with bin sizes ranging from 50-2000m.

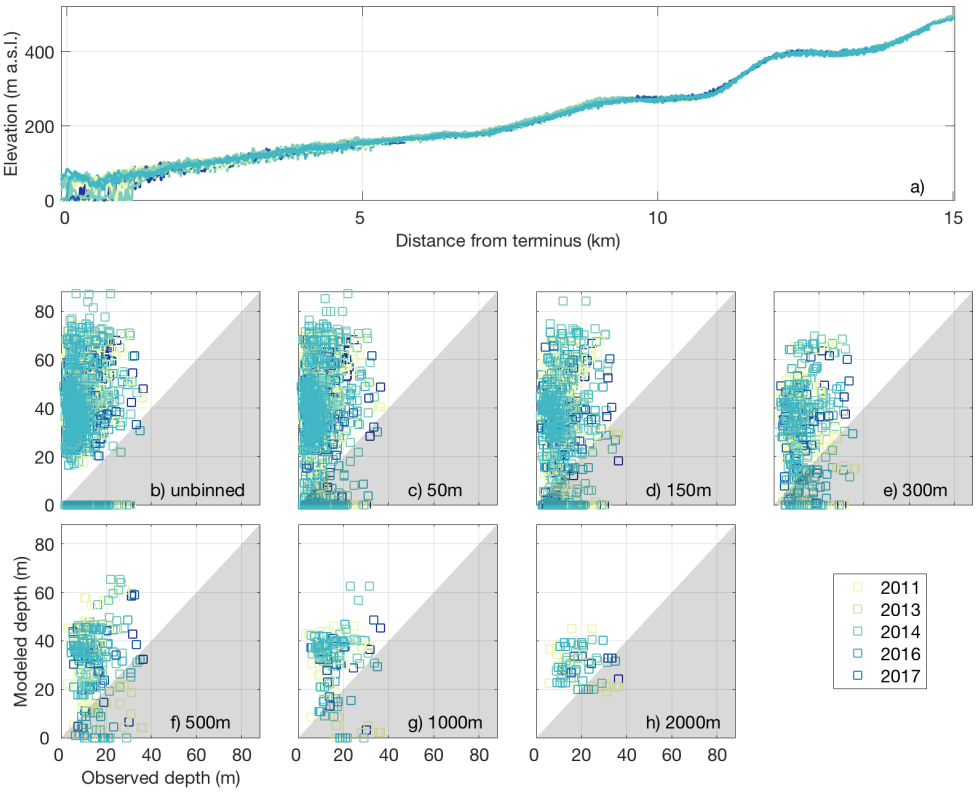

Figure S13: Upernavik Isstrøm (Sermeq) crevasse depth data. The legend indicates the observation year for all panels. a) Elevation profile time series extracted along the Operation IceBridge swath. b-h) Scatterplots of observed crevasse depths plotted against modeled crevasse depths. Points that fall in the white (gray) region represent model over-estimates (under-estimates) of the observed depths. All observations are shown in b whereas the maximum observed and median modeled depths within along-flow bins are shown in c-h, with bin sizes ranging from 50-2000m.

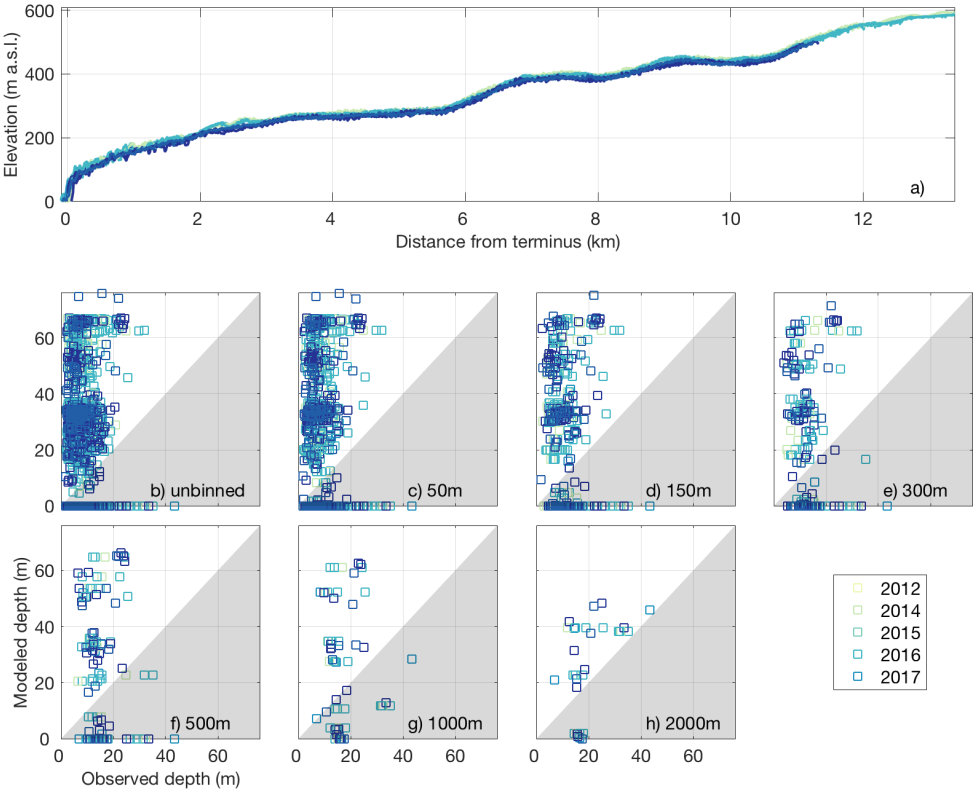

Figure S14: Umiammakku Sermiat crevasse depth data. The legend indicates the observation year for all panels. a) Elevation profile time series extracted along the Operation IceBridge swath. b-h) Scatterplots of observed crevasse depths plotted against modeled crevasse depths. Points that fall in the white (gray) region represent model over-estimates (under-estimates) of the observed depths. All observations are shown in b whereas the maximum observed and median modeled depths within along-flow bins are shown in c-h, with bin sizes ranging from 50-2000m.

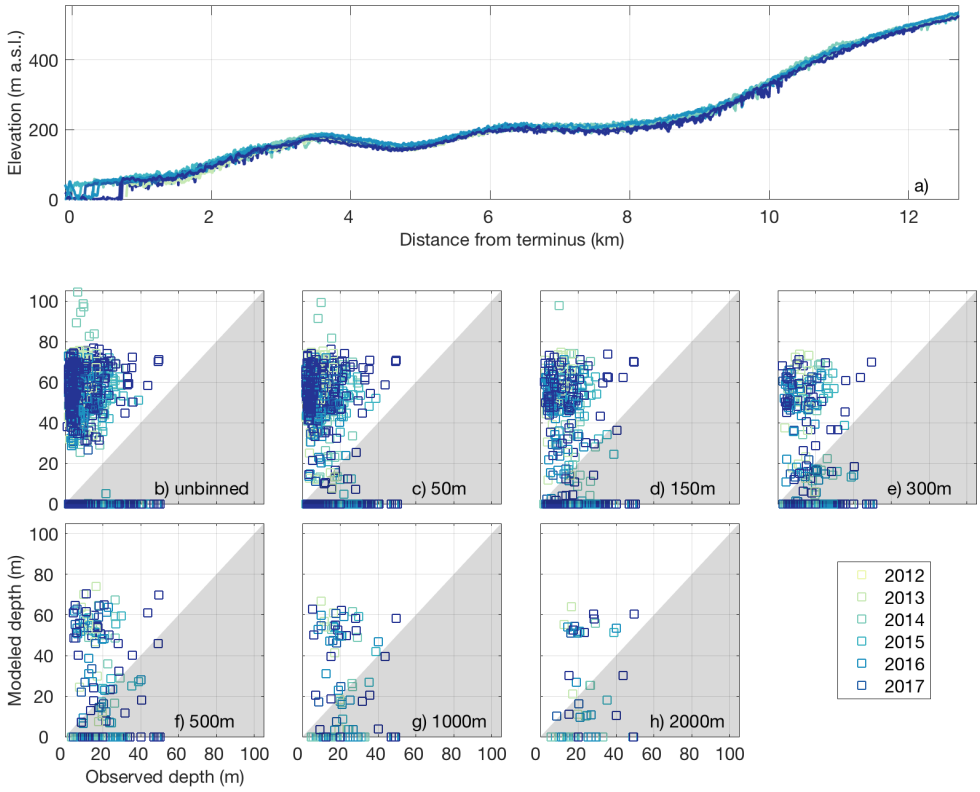

Figure S15: Rink Isbræ (Kangilliup Sermia) crevasse depth data. The legend indicates the observation year for all panels. a) Elevation profile time series extracted along the Operation IceBridge swath. b-h) Scatterplots of observed crevasse depths plotted against modeled crevasse depths. Points that fall in the white (gray) region represent model over-estimates (under-estimates) of the observed depths. All observations are shown in b whereas the maximum observed and median modeled depths within along-flow bins are shown in c-h, with bin sizes ranging from 50-2000m.

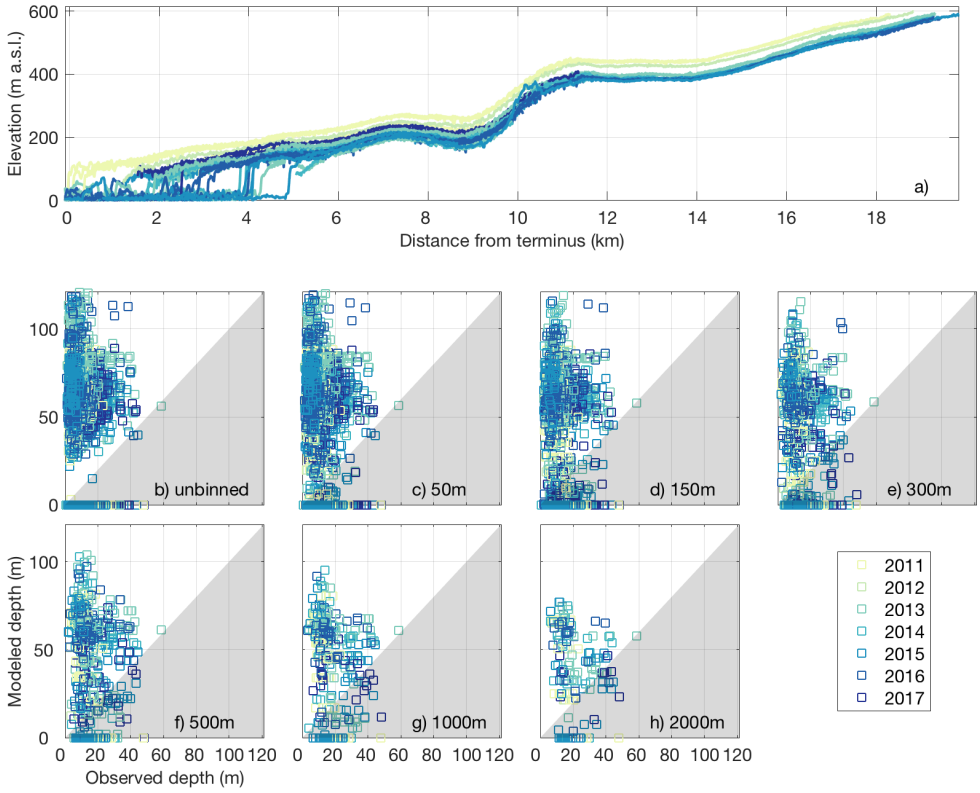

Figure S16: Jakobshavn Isbræ (Sermeq Kujalleq) crevasse depth data. The legend indicates the observation year for all panels. a) Elevation profile time series extracted along the Operation IceBridge swath. b-h) Scatterplots of observed crevasse depths plotted against modeled crevasse depths. Points that fall in the white (gray) region represent model over-estimates (under-estimates) of the observed depths. All observations are shown in b whereas the maximum observed and median modeled depths within along-flow bins are shown in c-h, with bin sizes ranging from 50-2000m.

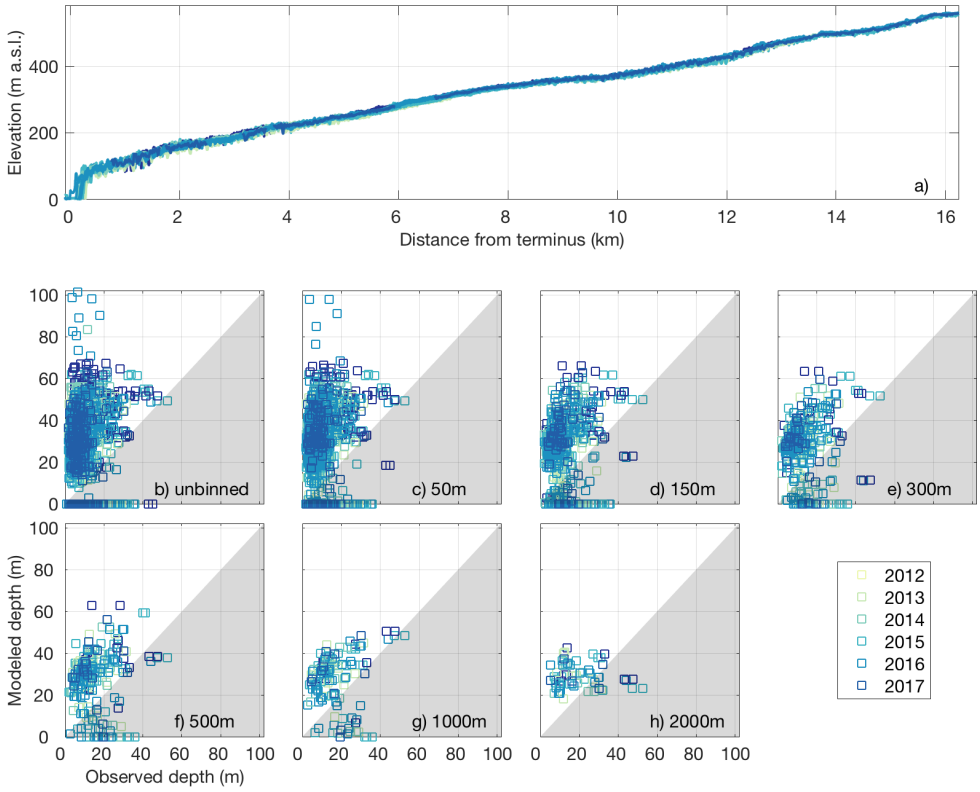

Figure S17: Heimdal Gletsjer crevasse depth data. The legend indicates the observation year for all panels. a) Elevation profile time series extracted along the Operation IceBridge swath. b-h) Scatterplots of observed crevasse depths plotted against modeled crevasse depths. Points that fall in the white (gray) region represent model over-estimates (under-estimates) of the observed depths. All observations are shown in b whereas the maximum observed and median modeled depths within along-flow bins are shown in c-h, with bin sizes ranging from 50-2000m.

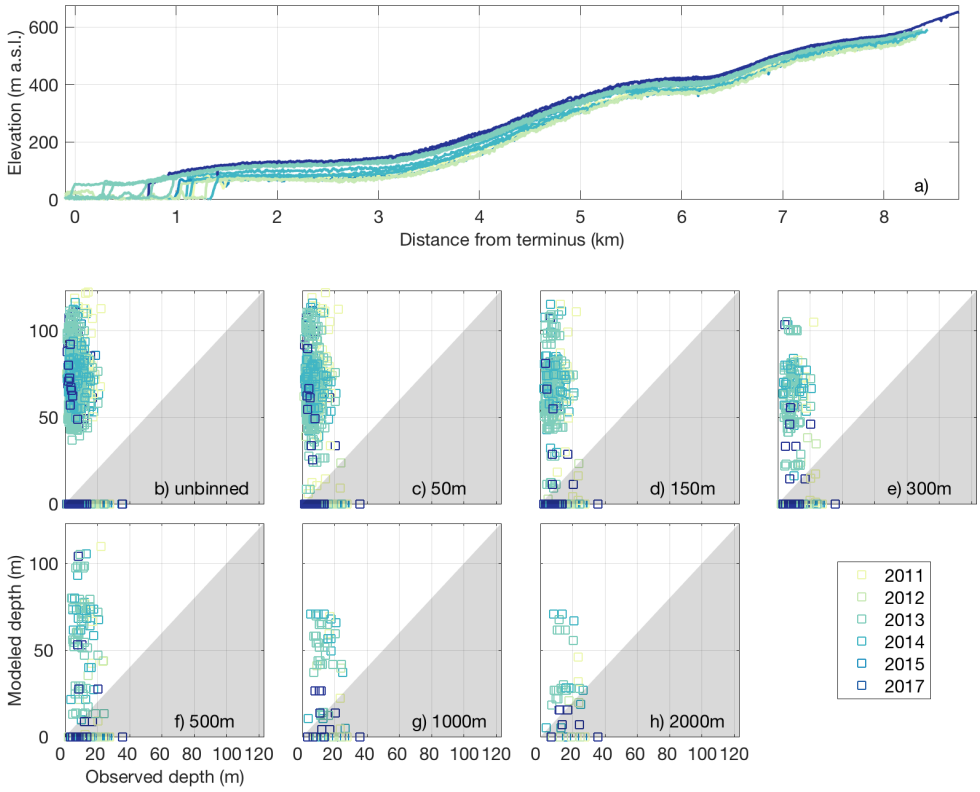

Figure S18: Kogr Bugt Gletsjer crevasse depth data. The legend indicates the observation year for all panels. a) Elevation profile time series extracted along the Operation IceBridge swath. b-h) Scatterplots of observed crevasse depths plotted against modeled crevasse depths. Points that fall in the white (gray) region represent model over-estimates (under-estimates) of the observed depths. All observations are shown in b whereas the maximum observed and median modeled depths within along-flow bins are shown in c-h, with bin sizes ranging from 50-2000m.

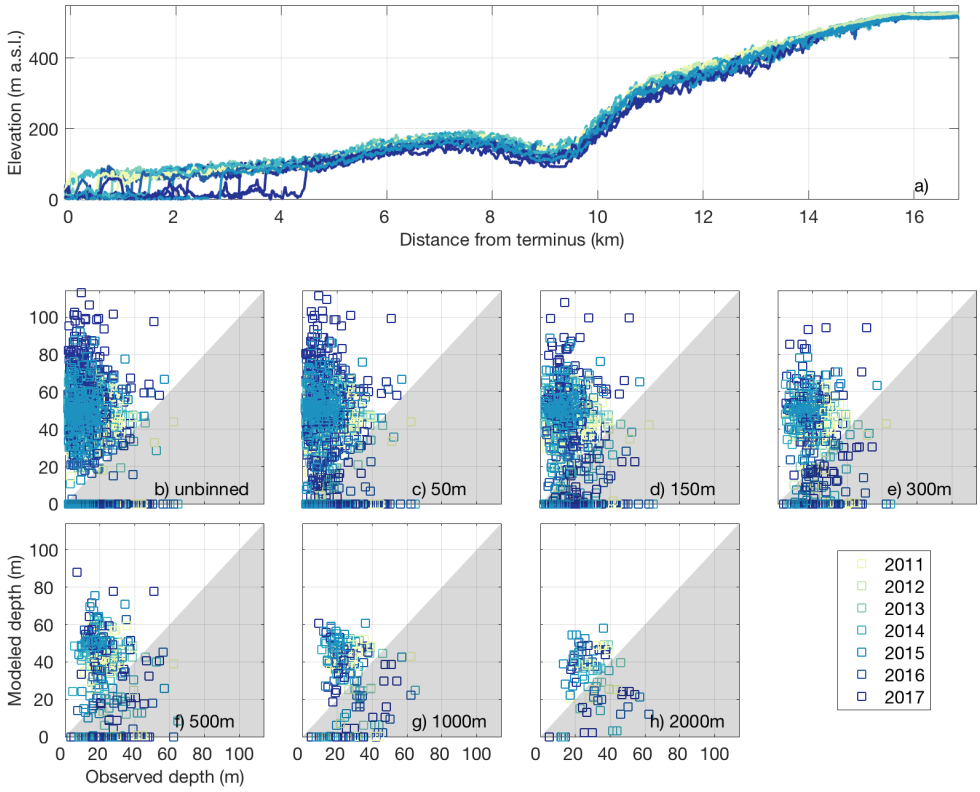

Figure S19: Helheim Gletsjer crevasse depth data. The legend indicates the observation year for all panels. a) Elevation profile time series extracted along the Operation IceBridge swath. b-h) Scatterplots of observed crevasse depths plotted against modeled crevasse depths. Points that fall in the white (gray) region represent model over-estimates (under-estimates) of the observed depths. All observations are shown in b whereas the maximum observed and median modeled depths within along-flow bins are shown in c-h, with bin sizes ranging from 50-2000m.

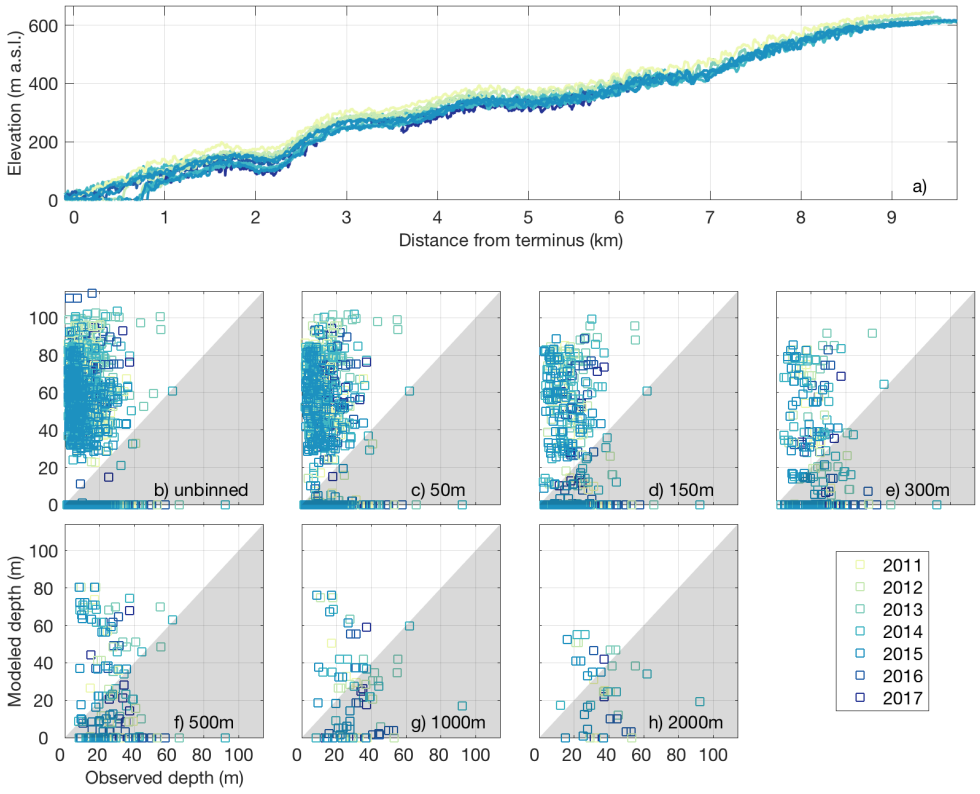

Figure S20: Midgård Gletsjer crevasse depth data. The legend indicates the observation year for all panels. a) Elevation profile time series extracted along the Operation IceBridge swath. b-h) Scatterplots of observed crevasse depths plotted against modeled crevasse depths. Points that fall in the white (gray) region represent model over-estimates (under-estimates) of the observed depths. All observations are shown in b whereas the maximum observed and median modeled depths within along-flow bins are shown in c-h, with bin sizes ranging from 50-2000m.

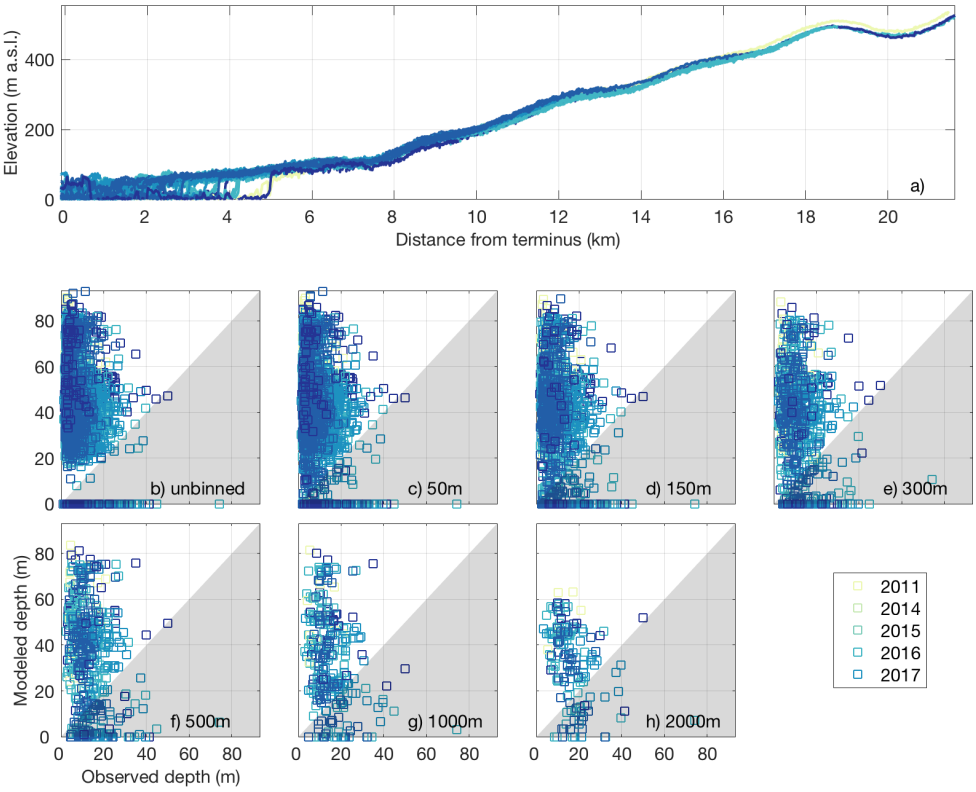

Figure S21: Kangerlussuaq Gletsjer crevasse depth data. The legend indicates the observation year for all panels. a) Elevation profile time series extracted along the Operation IceBridge swath. b-h) Scatterplots of observed crevasse depths plotted against modeled crevasse depths. Points that fall in the white (gray) region represent model over-estimates (under-estimates) of the observed depths. All observations are shown in b whereas the maximum observed and median modeled depths within along-flow bins are shown in c-h, with bin sizes ranging from 50-2000m.

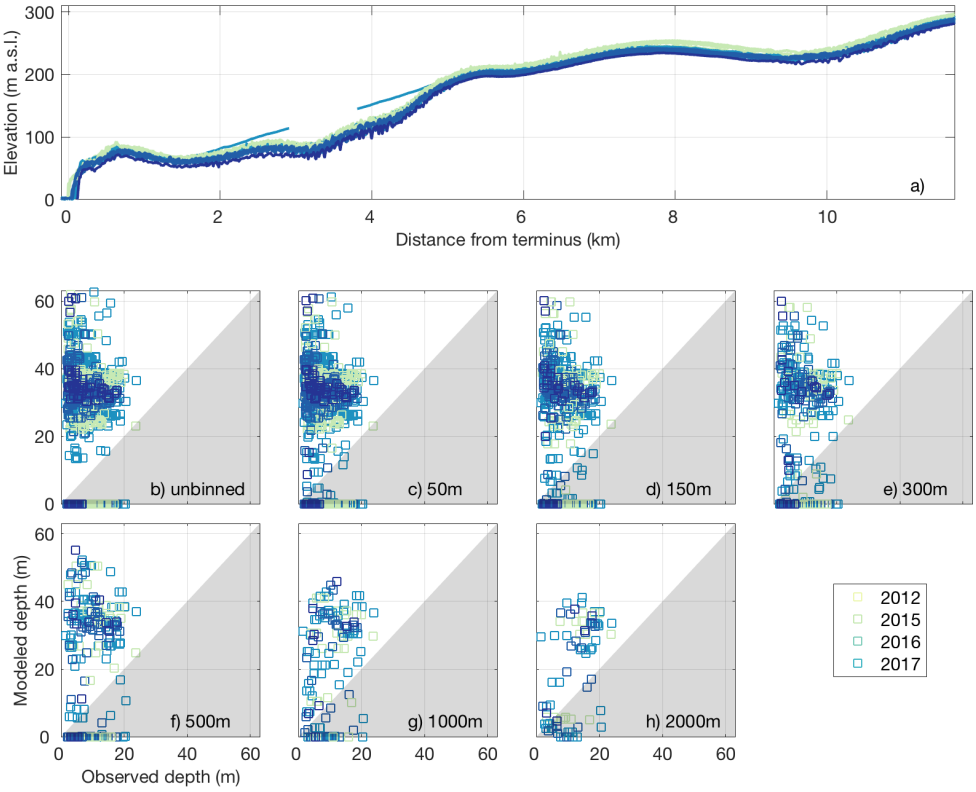

Figure S22: Dendrit Gletsjer crevasse depth data. The legend indicates the observation year for all panels. a) Elevation profile time series extracted along the Operation IceBridge swath. b-h) Scatterplots of observed crevasse depths plotted against modeled crevasse depths. Points that fall in the white (gray) region represent model over-estimates (under-estimates) of the observed depths. All observations are shown in b whereas the maximum observed and median modeled depths within along-flow bins are shown in c-h, with bin sizes ranging from 50-2000m.

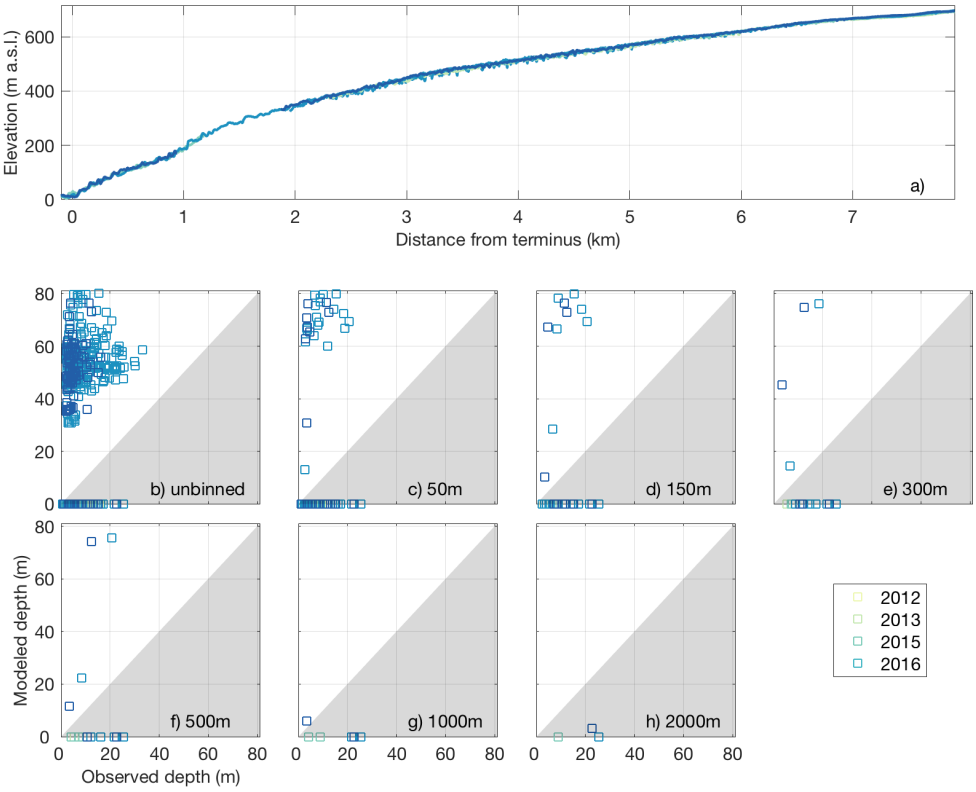

Figure S23: Magga Dan Gletsjer crevasse depth data. The legend indicates the observation year for all panels. a) Elevation profile time series extracted along the Operation IceBridge swath. b-h) Scatterplots of observed crevasse depths plotted against modeled crevasse depths. Points that fall in the white (gray) region represent model over-estimates (under-estimates) of the observed depths. All observations are shown in b whereas the maximum observed and median modeled depths within along-flow bins are shown in c-h, with bin sizes ranging from 50-2000m.

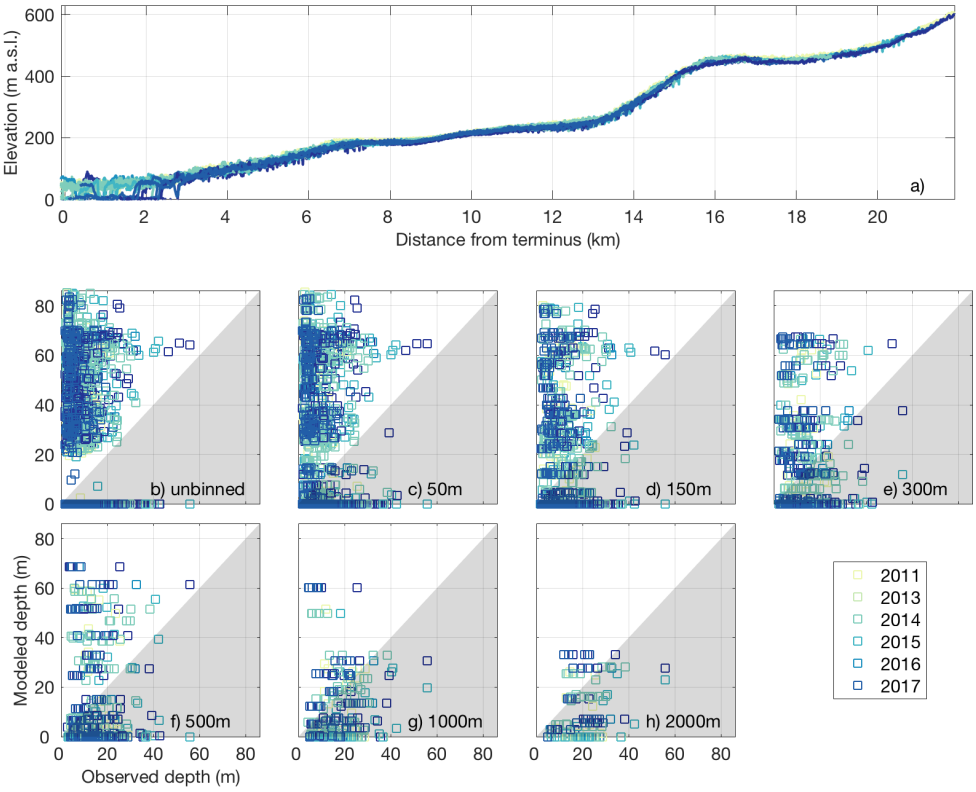

Figure S24: Daugaard Jensen Gletsjer crevasse depth data. The legend indicates the observation year for all panels. a) Elevation profile time series extracted along the Operation IceBridge swath. b-h) Scatterplots of observed crevasse depths plotted against modeled crevasse depths. Points that fall in the white (gray) region represent model over-estimates (under-estimates) of the observed depths. All observations are shown in b whereas the maximum observed and median modeled depths within along-flow bins are shown in c-h, with bin sizes ranging from 50-2000m.

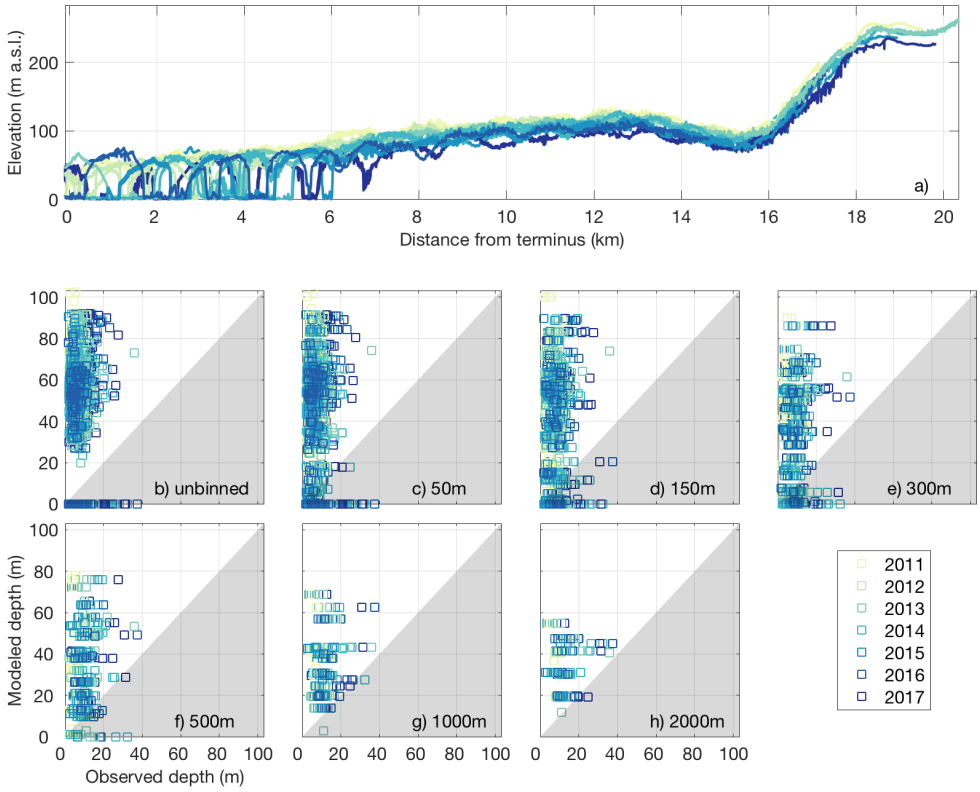

Figure S25: Zachariae Isstrøm crevasse depth data. The legend indicates the observation year for all panels. a) Elevation profile time series extracted along the Operation IceBridge swath. b-h) Scatterplots of observed crevasse depths plotted against modeled crevasse depths. Points that fall in the white (gray) region represent model over-estimates (under-estimates) of the observed depths. All observations are shown in b whereas the maximum observed and median modeled depths within along-flow bins are shown in c-h, with bin sizes ranging from 50-2000m.

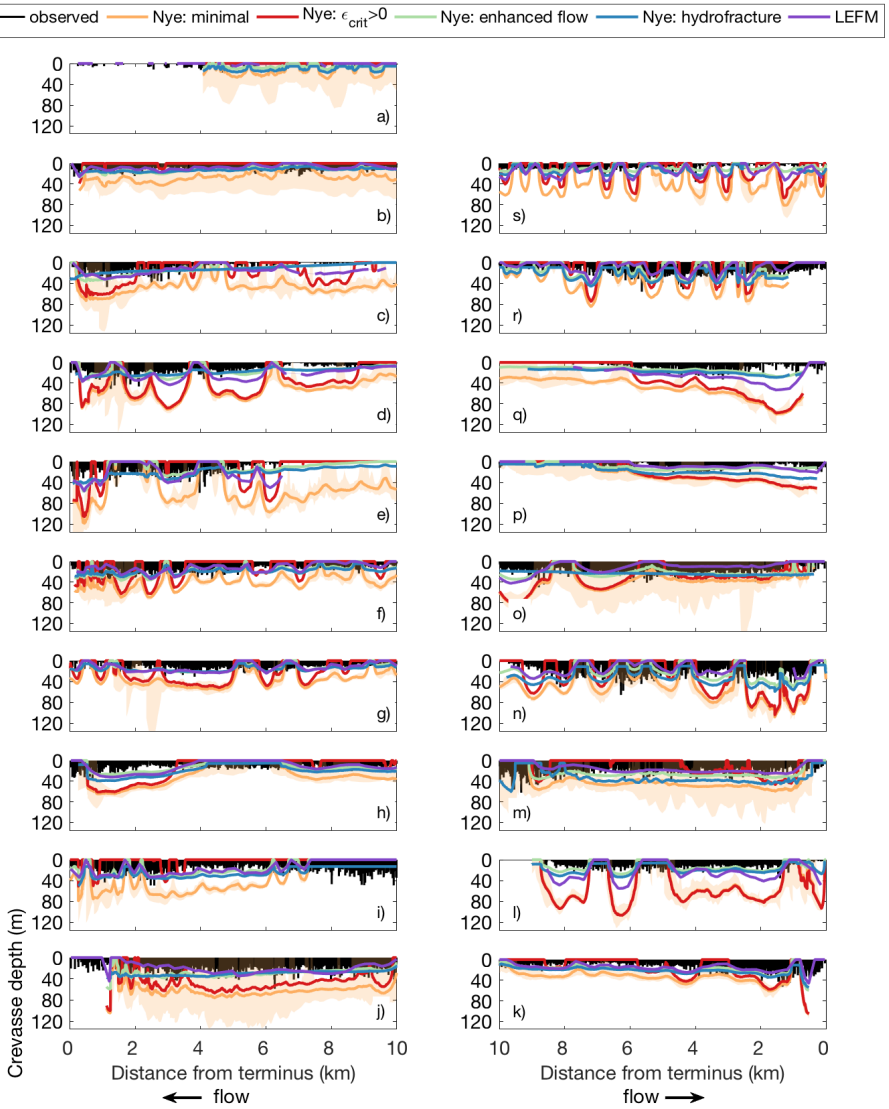

Figure S26: Crevasse depth profiles over the seaward-most 10km of each glacier. Observed crevasse depths are in black. Modeled depths using the minimal (orange), non-zero strain rate threshold (red), parameterized flow enhancement (green), and parameterized water depth (blue) versions of the Nye formulation for crevasse depth are plotted using the median strain rate profile. Temporal variability in the crevasse depths from the minimal model are shown as orange shading. The purple lines show the LEFM-modeled crevasse depths with the geometry-dependent stress intensity scaling factor calculated from observations. Panels are organized geographically, as in Figure S2.

2 Tables

		search window widths (m)	
		30,60,90	45,90,135
detrending window width (m)	350	350; 30,60,90	350; 45,90,135
	450	450; 30,60,90	450; 45,90,135
	500	500; 30,60,90	500; 45,90,135
	550	550; 30,60,90	550; 45,90,135
	650	650; 30,60,90	650; 45,90,135
	800	800; 30,60,90	800; 45,90,135

Table S1: Window sizes for automated crevasse identification.

5